

# Losses in single-mode silicon-on-insulator strip waveguides and bends

Yurii A. Vlasov and Sharee J. McNab

IBM T.J. Watson Research Center, Yorktown Heights, NY 10536

[yvlasov@us.ibm.com](mailto:yvlasov@us.ibm.com)

**Abstract:** We report the fabrication and accurate measurement of propagation and bending losses in single-mode silicon waveguides with submicron dimensions fabricated on silicon-on-insulator wafers. Owing to the small sidewall surface roughness achieved by processing on a standard 200mm CMOS fabrication line, minimal propagation losses of  $3.6 \pm 0.1$  dB/cm for the TE polarization were measured at the telecommunications wavelength of  $1.5 \mu\text{m}$ . Losses per  $90^\circ$  bend are measured to be  $0.086 \pm 0.005$  dB for a bending radius of  $1 \mu\text{m}$  and as low as  $0.013 \pm 0.005$  dB for a bend radius of  $2 \mu\text{m}$ . These record low numbers can be used as a benchmark for further development of silicon microphotonic components and circuits.

©2004 Optical Society of America

OCIS codes: (230.7370) Waveguides; (250.5300) Photonic integrated circuits

---

## References and Links

1. Y. Hibino, "Silica-Based Planar Lightwave Circuits and Their Applications," MRS Bulletin May 2003, p.365 (2003)
2. T. Shibata, M. Okuno, T. Goh, T. Watanabe, M. Yasu, M. Itoh, M. Ishii, Y. Hibino, A. Sugita, and A. Himeno, "Silica-Based Waveguide-Type 16x16 Optical Switch Module Incorporating Driving Circuits," IEEE Phot. Techn. Lett. **15**, 1300 (2003).
3. G.-L. Bona, R. Germann, and B. J. Offrein, "SiON high refractive-index waveguide and planar lightwave circuits," IBM J. Res.Develop. **47**, 239 (2003).
4. S. J. McNab, N. Moll and Yu. A. Vlasov, "Ultra-low loss photonic integrated circuit with membrane-type photonic crystal waveguides," Opt. Express **11**, 2927 (2003).  
<http://www.opticsexpress.org/abstract.cfm?URI=OPEX-11-22-2927>
5. K. K. Lee, D. R. Lim, H.-C. Luan, A. Agarwal, J. Foresi, and L. C. Kimerling "Effect of size and roughness on light transmission in a Si/SiO<sub>2</sub> waveguide: Experiments and model," Appl. Phys. Lett., **77**, 1617 (2000).
6. K. K. Lee, D. R. Lim, and L. C. Kimerling, "Fabrication of ultralow-loss Si/SiO waveguides by roughness reduction," Opt. Lett., **26**, 1888 (2001).
7. K.K.Lee, "Transmission and routing of optical signals in on-chip waveguides for silicon microphotronics," PhD thesis, MIT (2001).
8. D.R.Lim, "Device integration for silicon microphotronics platforms," PhD thesis, MIT (2000);
9. A. Sakai, G. Hara, and T. Baba, "Propagation characteristics of ultrahigh  $\Delta$  optical waveguide on silicon-on-insulator substrate," Jpn. J. Appl. Phys. Part 2, **4B**, L383 (2001).
10. P. Dumon, W. Bogaerts, J. Van Campenhout, V. Wiaux, J. Wouters, S. Beckx, R. Baets, "Low-loss photonic wires and compact ring resonators in silicon-on-insulator," LEOS Benelux Annual Symposium 2003, Netherlands, (2003)
11. T. Tsuchizawa, T. Watanabe, E. Tamechika, T. Shoji, K. Yamada, J. Takahashi, S. Uchiyama, S. Itabashi and H. Morita, "Fabrication and evaluation of submicron-square Si wire waveguides with spot-size converters", Paper TuU2 presented at LEOS Annual Meeting, p.287, Glasgow, UK (2002).
12. R. U. Ahmad, F. Pizzuto, G. S. Camarda, R. L. Espinola, H. Rao, and R. M. Osgood, Jr., "Ultracompact Corner-Mirrors and T-Branched in Silicon-on-Insulator", IEEE Photon. Techn. Lett., **14**, 65 (2002).
13. V.Almeida, R. Panepucci, and M.Lipson, "Nanotaper for compact mode conversion," Opt. Lett. **28**, 1302 (2002).
14. T. Shoji, T. Tsuchizawa, T. Watanabe, K. Yamada, H. Morita, "Low loss mode size converter from  $0.3 \mu\text{m}$  square Si wire waveguides to singlemode fibers," Electron. Lett., **38**, 1669 (2002).
15. P. K. Tien, "Light waves in thin films and integrated optics," Appl. Opt., **10**, 2395 (1971)
16. D. Marcuse, "Mode conversion caused by surface imperfections of a dielectric slab waveguide," Bell Syst. Tech. J. **48**, 3187 (1969).
17. F. P. Payne and J. P. R. Lacey, "A theoretical analysis of scattering loss from planar optical waveguides," Opt. Quantum Electron. **26**, 977 (1994).

## 1. Introduction

Integration of discrete photonic components into a single chip is a long-standing goal of integrated optics. In current mature silica-on-silicon technology the waveguide is formed in a silica layer by doping it with P or Ge atoms [1]. Impressive levels of integration have already been demonstrated, for example, a 16x16 switch array on a single 6 inch silicon wafer [2]. Further increases in integration density with this technology are restricted however, by the large minimal bending radius of silica waveguides which is of the order of a few cms. A significant step toward much denser integration has been demonstrated with silicon oxynitride (SiON) technology [3]. A much higher index contrast in the order of 3.3% is introduced between the core of the SiON waveguide and silica cladding, which allows the minimum bending radius to be reduced to below 1mm. Further aggressive scaling is possible with silicon-on-insulator (SOI) technology, where the waveguide is formed in a thin silicon layer. Extremely high refractive index contrast between the silicon core ( $n=3.5$ ) and silica cladding (1.45) allows the waveguide core to be shrunk down to a submicron cross-section, while still maintaining single mode propagation at 1.3-1.5 micron telecommunications wavelengths. Such extreme light confinement allows the minimal bending radius to be reduced to the micron range, opening an avenue to realize ultra-dense photonic integrated circuits on a single silicon chip [4].

Such extreme light confinement in submicron SOI strip waveguides also results in significantly enhanced propagation losses due to increased interaction of the waveguiding mode with the sidewall surface roughness. Extensive experimental studies have shown that surface roughness is responsible for high propagation losses, which can become prohibitive for building dense integrated circuits [5-11]. The same surface roughness is also responsible for high bending losses typically in the order of a dB per 90 degree bend [7-12].

In this paper we report the fabrication and accurate measurement of losses in single-mode SOI strip waveguides and bends processed on a standard 200mm CMOS fabrication line.

## 2. Experimental

### 2.1. Design and fabrication

Devices were fabricated on SOI Unibond 200 mm wafers manufactured by SOITEC with 220 nm of lightly p-doped Si on a 2 $\mu$ m buried oxide (BOX) layer. The thick oxide serves to optically isolate the circuit from the substrate, reducing losses due to substrate leakage. A 50 nm thick oxide was deposited on the wafers via low pressure chemical vapor deposition to act as a hard mask for subsequent etching. Wafers were coated with photoresist and exposed by electron beam lithography using Leica's VB6-HR commercial 100 keV system. The exposed wafers were etched in a standard 200mm CMOS line at IBM Watson Research Center. The resist pattern was first transferred to the oxide hard mask using a CF<sub>4</sub>/CHF<sub>3</sub>/Ar chemistry. The resist was then removed and the patterned oxide used as a mask to transfer the pattern to the Si layer via an HBr-based etch. Further details of the fabrication are reported elsewhere [4]. Strip silicon waveguides were defined by etching two parallel 2 $\mu$ m wide slots in silicon layer down to the BOX layer as shown in Fig. 1. The resulting waveguide with core cross-section of 445x220nm can support a single TE mode in 1350-1750nm wavelengths region.

For efficient and reproducible coupling from a fiber to single-mode waveguides spot-size converters based on inverted taper geometry [4,13,14] were defined on each side of the waveguides as described in Ref.[4].

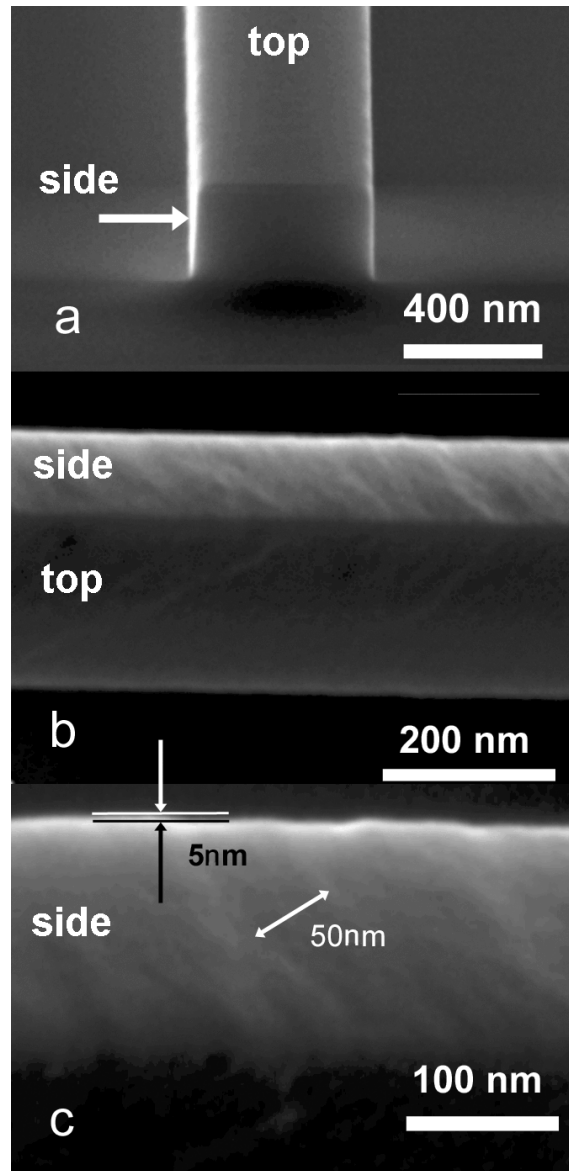


Fig. 1. SEM images of a single-mode strip waveguide with 445x220nm core cross-section at different orientations to show the sidewall quality.

Propagation loss measurements were made with the cut-back method whereby a set of waveguides of varying lengths from 4.7mm to 21mm were defined. The serpentine layout illustrated schematically in the inset of Fig. 2 was used so that all the waveguides had their in- and out-coupling ports aligned in each sample. Each waveguide in a series contains 8 identical bends with a bend radius  $R=5\mu\text{m}$ .

To measure waveguide bending losses two additional sets of waveguides were designed. One set contains waveguides with 10 bends folded in a serpentine pattern and another set with 20 bends. The total length of each folded waveguide is fixed at 4.5mm. Each set contains three different bend radii,  $R=5\mu\text{m}$ ,  $2\mu\text{m}$  and  $1\mu\text{m}$ . In addition to the folded waveguides a straight waveguide of 4.2mm length without bends was included for comparison and normalization.

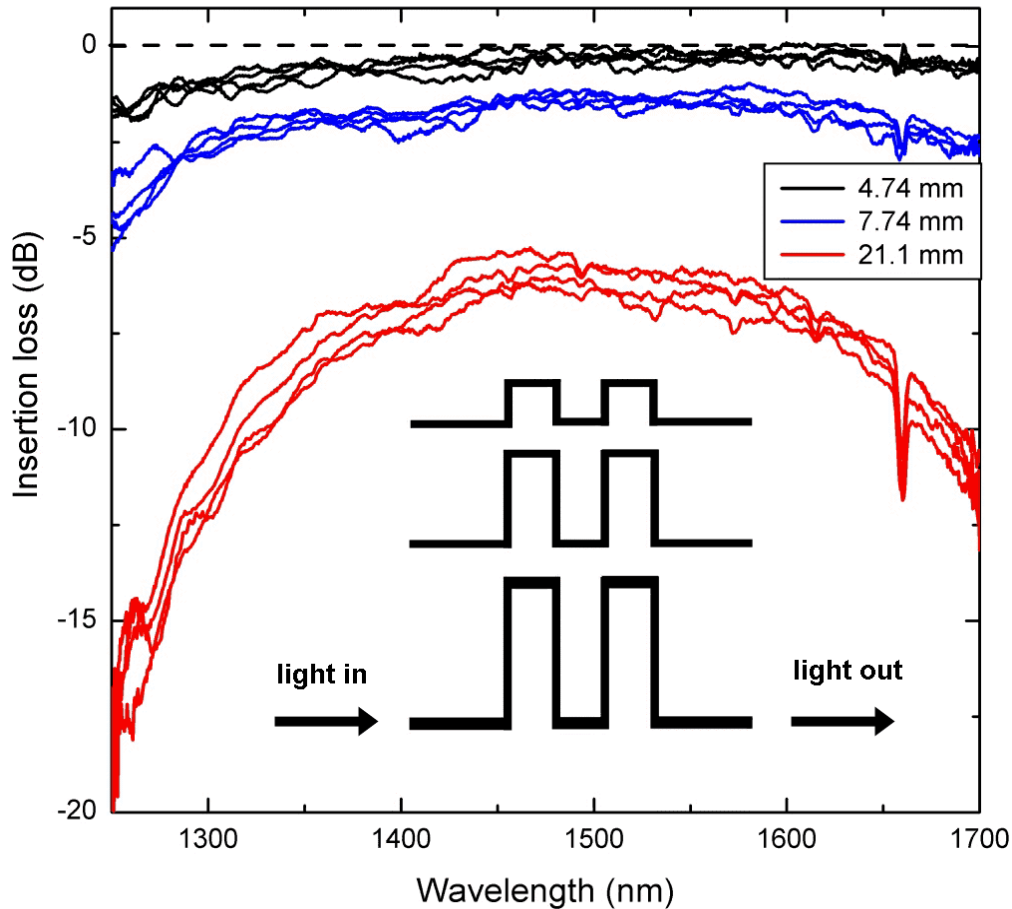


Fig. 2. Transmission spectra of a set of 445x220nm SOI strip waveguides of different lengths measured for TE-polarized light. Spectra are normalized on transmission through a straight 4.2mm long strip waveguide without bends. Inset: schematic of the serpentine waveguide layout to obtain different waveguide lengths with aligned input and output ports.

Finally individual chips containing all three sets of devices repeated in 4 writing fields were cleaved from both sides to enable edge fiber coupling. Since in a serpentine layout both in- and out-coupling spot-size converters are aligned the resulting cleaved chip has 88 coupling ports from each side, which allows the different devices to be measured consistently by simply shifting the chip using the XYZ translation stage.

## 2.2. Experimental set-up

The device under test (DUT) was mounted on a XYZ translational stage. Light from the broadband LED source with a bandwidth spanning 1200 to 1700nm was coupled to a polarization maintaining (PM) fiber and directed through a polarization controller before being coupled to the DUT via a tapered and microlensed PM fiber. The fiber tip produces a spot with a beam waist of 2.1 $\mu\text{m}$  with minimal mixing of TE-TM modes (rejection ratio of over 30-40dB). After passing through the DUT the light was collected by a tapered SMF fiber with beam waist of 1.85  $\mu\text{m}$  and the transmission analyzed by an optical spectrum analyzer. The input and output fibers are mounted on XYZ micrometer piezo-stages for precision alignment with respect to the DUT. Further details of the experimental set-up for measuring the transmission spectra are published elsewhere [4].

### 3. Propagation losses in single-mode 445x220nm strip waveguides

#### 3.1 Propagation loss measurements by a cut-back method

Figure 2 presents a set of transmission spectra measured for TE polarization on the first set of devices that vary the waveguide length from 4.7 mm to 21mm, while maintaining a fixed number of bends (8) with a  $R=5\mu\text{m}$ . In order to remove the spectral dependence induced by the coupling coefficient of the spot-size converters each spectrum is normalized on the transmission through a straight 4.2mm length waveguide without bends. The absolute transmission spectrum of the latter is identical to that already published in Ref. [4].

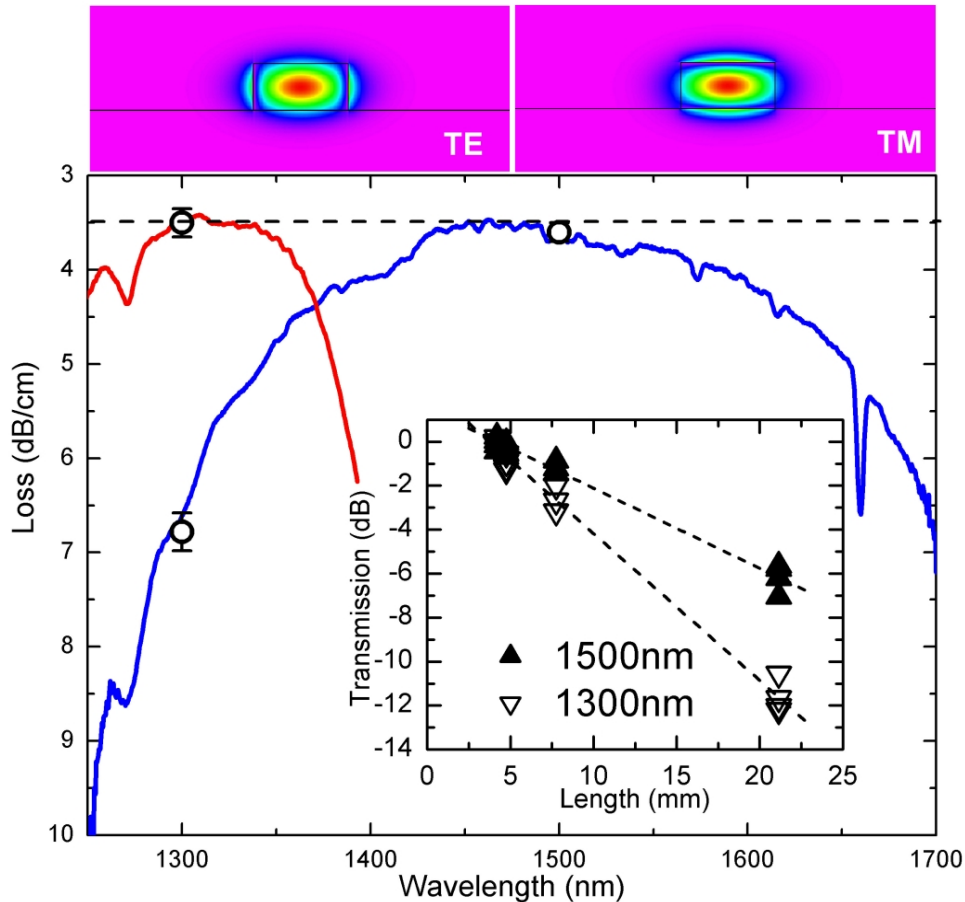


Fig. 3. Loss spectrum derived from the results of Fig. 2 for 445x220nm SOI strip waveguide. Blue (red) line corresponds to TE (TM) polarizations. Circles represent results from the loss measurements obtained by fitting the slope as shown in the inset. Inset: TE transmission as a function of the waveguide length for two different wavelengths of 1300 and 1500nm. Top panel shows the mode profile for TE- and TM-like modes of the waveguide at 1300nm wavelengths.

The cut-back method for measurements of propagation losses is based on a comparison of transmission through waveguides of different lengths and fitting the length dependence assuming identical coupling conditions and identical surface roughness. It is also assumed that the total bending losses in 8 bends ( $R=5\mu\text{m}$ ) is negligible (see results of Sect.4 below). It can be seen from Fig. 2 that the transmission curves measured for devices of the same length in the 4 different fields closely coincide demonstrating good repeatability in coupling. Uncertainty of coupling to different devices, measured independently on 10 identical straight

waveguides, does not exceed 0.1dB standard deviation. The standard deviation of the scattering of the transmission for the 4.74mm and 7.74 mm waveguides is about 0.4dB. For the longer 21mm devices the scatter in the transmission is increased to about 1dB indicating that there are some variations in the waveguides that begin to dominate here. The experimental uncertainty of 1dB can be used to estimate the upper limit of the error in determination of propagation losses by a cut-back method. Taking into account that the longest device in the series is 21mm long and the transmission difference between devices of different length can be measured with 1dB uncertainty, the upper limit of the error in the loss figure can be estimated to be smaller than 0.5dB/cm; this uncertainty can be further reduced by statistical averaging.

Measurements of the transmission coefficient as a function of the length for two fixed wavelengths of 1300nm and 1500nm are presented in the inset of Fig. 3. Linear fitting gives loss numbers of  $3.6 \pm 0.1$ dB/cm for 1500nm and  $6.8 \pm 0.2$ dB/cm for 1300nm. Analogous measurements made for TM polarized light at 1300nm showed losses of  $3.5 \pm 0.1$ dB/cm. As the transmission is measured for wavelengths from 1200-1700nm it is possible to extract not only the loss figure at fixed wavelengths but also over the whole spectrum. The transmission spectrum for 21mm long waveguide averaged over 4 measurements is subtracted (in a dB scale) from the averaged spectrum of 4.7mm long device and divided by the difference in length. The resulting curves for both TE and TM polarizations are shown in Fig. 3. It is seen that the loss figures determined from the linear fit (denoted by circles) calculated at fixed wavelengths of 1300nm and 1500nm for the full range of lengths coincide with the results calculated for the loss spectrum.

### 3.2. Analysis of the results

The measured loss number for the TE mode at 1500nm wavelengths closely coincides with our recent measurements of propagation losses in strip waveguides of similar cross-section of 465x220nm, which showed  $3.5 \pm 2$ dB/cm [4]. However, the experimental method used in Ref.[4] based on capturing vertically scattered IR light along the length of the waveguide, significantly overestimated losses at 1300nm wavelengths as  $12.5 \pm 1$ dB/cm. Indeed, as it is seen from the loss spectrum in Fig. 3, the sharp enhancement of losses is evident at wavelengths around 1300nm. It can be argued then that most of the vertically scattered light captured by the IR camera in experiments of Ref.[4] is coming from the short-wavelength wing of the broadband (70nm FWHM) spectrum of the LED source and, correspondingly, the measured loss value should be assigned to wavelengths shorter than 1300nm in accordance with the present measurements. As it is seen from Fig. 3 the loss spectrum is relatively smooth around 1500nm wavelength and all light from the LED with 70nm bandwidth is scattered vertically with similar efficiency thus minimizing the error in loss determination. Only the measurements of spectral dependence of losses, as it is done in the present work, can be used to fully characterize the loss mechanisms.

The simple analytical model proposed by Tien [15] shows that propagation loss  $\alpha$  is defined as:

$$\alpha = \frac{4\sigma^2 h^2}{\beta(r+2/p)} = \frac{\sigma^2 k_0^2 h}{\beta} \cdot \frac{E_s^2}{\int E^2 dx} \cdot \Delta n^2 \quad (1)$$

where  $\sigma$  is the interface roughness,  $t$  is the waveguide thickness,  $k_0$  is the free space wavenumber,  $\beta$  is modal propagation constant,  $\Delta n$  is the difference between the refractive indices of the core and cladding, while  $h$  and  $p$  are the transverse propagation constants in the core and cladding, respectively. It is seen that loss is proportional to  $E_s^2 / \int E^2 dx$ , the normalized electric field intensity at the core/cladding interface and to the square of interface roughness  $\sigma$ .

The top and bottom interfaces in Unibond SOI wafers are nearly atomically flat and do not contribute significantly to scattering. The surface roughness of the sidewalls can be

roughly estimated from the SEM inspection of the etched sidewalls as shown in Fig. 1. While the amplitude of the roughness is too small to estimate the power spectrum, the amplitude and approximate mean distance between the surface fluctuations can be estimated to be below 5nm and of the order of 50nm, respectively.

Experimental results showed that for a fixed wavelength of 1300nm the losses of the TM mode are much smaller than the TE mode. This result directly demonstrates that the main source of propagation losses in our waveguides is the residual surface roughness on the etched sidewalls. Indeed, as it is seen from the top panel in Fig. 3, the TE mode profile is characterized by much higher electric field intensity at the sidewalls and correspondingly higher propagation losses. In contrast, the TM mode has a relatively small amplitude at the sidewalls, but much higher at the top and bottom interfaces.

The Marcuse, Payne and Lacey model [16,17], showed that for accurate loss calculations it is necessary to take into account not only the roughness standard deviation  $\sigma$ , but also the autocorrelation length  $L_c$ . According to this model, which was extended in Ref.5 to describe 3D waveguides, the propagation losses can be expected to be of the order or below 1-5dB/cm for the estimated above roughness amplitude (5nm amplitude corresponds to standard deviation  $\sigma \sim 2$ nm) and mean distance (assuming autocorrelation length  $L_c \sim 50$ nm). Although the model is derived for symmetric waveguides the results agree qualitatively with the experimentally measured loss figure.

The experimentally measured spectral dependence of losses for the TE polarization, shown in Fig. 3 by a black line has a relatively flat wavelength dependence and minimal losses around 1450-1500nm. Contribution of two scattering mechanisms can explain the observed dependence. Increase of losses at longer wavelengths can be explained by the vicinity of the long-wavelength TE mode cut-off around 1750nm. Near the cut-off the mode is much less confined and the interaction with the sidewall roughness is increased giving rise to enhanced losses of 5-8dB/cm around 1700nm. Significant increase of losses at shorter wavelengths, where the mode confinement is not changing significantly, can be explained by stronger scattering of the mode as the roughness amplitude is increased relative to the wavelength.

Spectral behavior of the TM mode losses is analogous. The long-wavelength cut-off of the fundamental TM mode was measured on straight waveguide to be located at 1400nm. The TM loss spectrum in Fig. 3 exhibit apparent cut-off around 1350nm shifted to shorter wavelengths due to increased propagation losses. At wavelengths shorter than 1250nm the losses are increasing again leaving the spectral region 1300-1350nm with minimal losses.

### 3.3. Comparison with literature results

Comparison with results in the literature is difficult because, as it is seen from the Eq. (1), losses depend strongly on a) cross-section of the waveguide core and b) on the wavelength of light for a given core size. The dependence of losses on the width of the single-mode waveguide is quasi-exponential reflecting strong enhancement of interaction of the mode with the sidewall surface with the decrease of the waveguide cross-section [5-9]. Correspondingly a fair comparison is possible only for waveguides of comparable cross-sections (comparable propagation constants) and for the analogous wavelengths corresponding to the spectral loss minimum. Table 1 attempts to summarize results from the existing literature.

Table 1. Comparison of propagation losses of the TE mode measured in single-mode SOI strip waveguides.

Reference	Height (nm)	Width (nm)	Loss (dB/cm)	Wave-length (nm)	Method	Note
This work	220	445	3.6±0.1	1500	cut-back	21mm long
[4]	220	465	3.5±2	1500	IR capture	4mm long
[13]	270	470	5±2	1550	Fabry-Perot	13mm long
[10]	220	400	33.8±1.7	1550	Fabry-Perot	1mm long
	220	450	7.4±0.9	1550		
	220	500	2.4±1.6	1550		
[11]	300	300	6	1550	cut-back	oxidation smoothing, 16mm long
	300	300	13	1550		
[9]	320	400	25±10	1550	Fabry-Perot	0.18mm long
[5-8]	200	500	32	1540	cut-back	silica cladding

Note that no additional processing following etching was attempted to further minimize surface roughness in this work. It has been successfully shown [6,7,11], for example, that oxidation smoothing of the sidewalls can significantly reduce the standard deviation of the roughness  $\sigma$  for the same  $L_c$ , leading to lower loss figures. As a side effect of oxidation the size of the silicon core of the waveguide is also considerably reduced, which if not compensated for will result in a decrease of the effective refractive index of the mode. A reduction in the mode effective index is largely responsible for the extremely low losses of 0.8dB/cm reported in Refs. [6,7], because the final thickness of the Si core was only 50nm. In this case waveguiding is most likely provided by a thick rib-shaped silica cladding, with the mode profile more closely resembling that of a large cross-sectional Ge-doped silica waveguide. The disadvantage of this approach is that the benefits of using a high index contrast system are lost such as small bending radii and high light confinement..

#### 4. Losses in small radius 90° waveguide bends

##### 4.1. Measurements of bending losses

For spectral measurements of the bending loss the transmission spectra were measured for two sets of waveguides: one with 10 and another with 20 bends. Each set contained bends with radii of  $R=5\mu\text{m}$ ,  $2\mu\text{m}$  and  $1\mu\text{m}$ . Assuming that light leakage in the bended waveguide is an exponential function of the number of bends, the bending loss spectra can be extracted from transmission spectra in a manner analogous to propagation loss spectra in Section 3. Transmission spectra for 10 and 20 bends were averaged over measurements from 4 devices and the difference taken and divided by 10 to obtain a loss figure per bend. Since the length of all waveguides is kept constant as 4.5mm, both the propagation loss and the coupling losses are cancelled out during this procedure. The resulting bending loss spectra for different radii are presented in Fig. 4 for both TE and TM modes.

It is seen that for bending radius  $R=5\mu\text{m}$  the bending loss of the TE mode lies within uncertainty interval  $\pm 0.005\text{dB/turn}$  defined by fluctuations of the loss spectrum. Decrease of the bend radius to  $R=2\mu\text{m}$  results in a small increase in bending loss, which can be estimated as  $0.013\pm 0.005\text{dB/turn}$  for a broad range of wavelengths 1325-1525nm. Such small losses are a direct result of very high mode confinement in single-mode SOI strip waveguides. Only for bends with radii as small as  $R=1\mu\text{m}$  do the bending losses become large enough to measure accurately. Even for these small bends the bending loss is  $0.086\pm 0.005\text{dB/turn}$  over most of the bandwidth of 1325-1525nm. At longer wavelengths, however, much higher bending losses of 0.2-0.3dB/turn can be observed. The increase in bending loss at longer wavelengths is expected as the mode approaches cut-off. The origin of dips seen in the spectrum at 1577nm and 1647nm is unclear. The resonance corresponds to a spatial periodicity of  $\sim 5\mu\text{m}$ , which we believe may have been inadvertently introduced during fabrication.



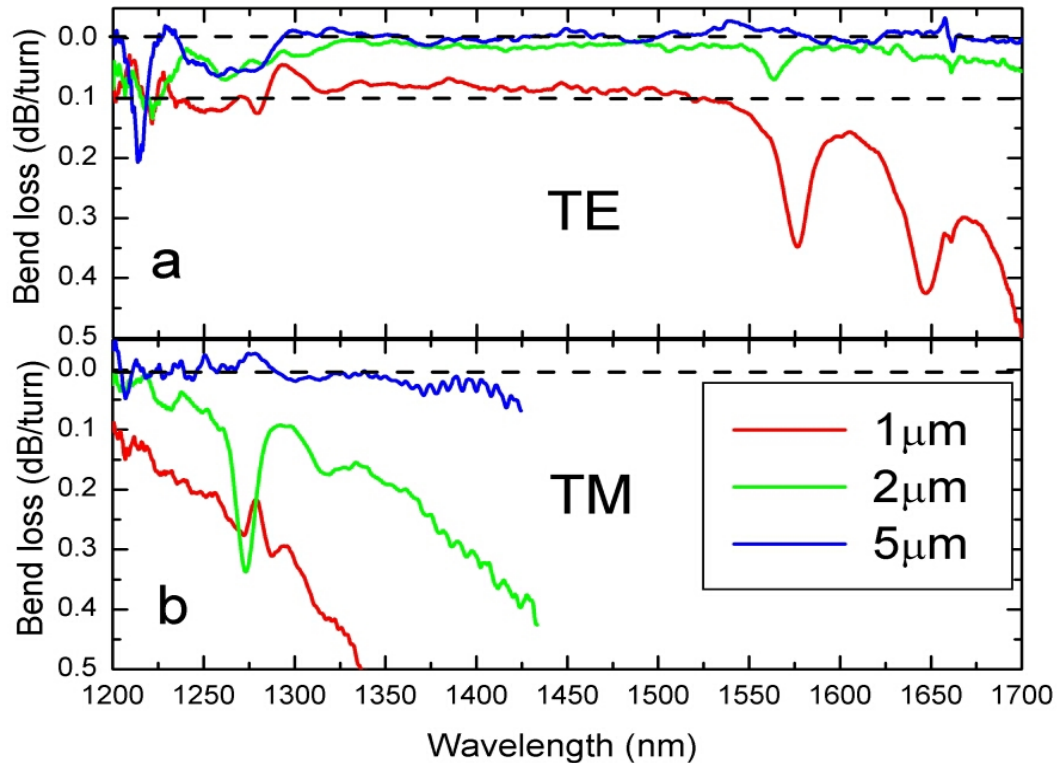


Fig. 4. Spectra of bending losses for TE (a) and TM (b) polarizations. Red, green and blue curves correspond to measurements of bends with radii  $R=1, 2,$  and  $5$  microns.

Bending loss spectra for the TM mode shows analogous behavior. For a bending radii  $R=5\mu\text{m}$  bending loss is negligible and lies within experimental uncertainty interval. Close to the fundamental cut-off at  $1400\text{nm}$  the bending loss increases substantially, especially for small bending radii of  $R=1\mu\text{m}$  and  $2\mu\text{m}$ . For example the bending loss at  $1325\text{nm}$  wavelength increases exponentially from  $0.16\text{dB/turn}$  to  $0.45\text{dB/turn}$  with the decrease of bending radius from  $R=2\mu\text{m}$  to  $1\mu\text{m}$ . However at  $1200\text{nm}$  wavelength far from the cut-off the loss is relatively small:  $0.015\pm 0.01\text{dB/turn}$  and  $0.1\pm 0.01\text{dB/turn}$  for  $R=2\mu\text{m}$  and  $1\mu\text{m}$ , respectively.

#### 4.2. Data analysis and comparison with literature results

When light is propagating in a curved waveguide the mode gets shifted toward the outer edge. In sharp strip waveguide bends this effect results in a possibility of mode radiation, reflection due to phase mismatch between the mode in the bend and in the straight section, and enhancement of losses due to increased interaction of the mode with the sidewall surface roughness. The simplest approximation to describe radiation loss [18] shows that bending loss  $\alpha$  is exponentially dependent on the bend radius  $R$ :

$$\alpha = K \cdot \exp(-cR), \text{ where } c = \beta(2\Delta n_{\text{eff}}/n_{\text{eff}})^{3/2} \quad (2)$$

, where  $K$  depends on the refractive indices of cladding and core and on waveguide thickness, and  $\beta$  is a modal propagation constant.  $\Delta n_{\text{eff}}$  is the difference between the modal effective index  $n_{\text{eff}}$  and the cladding index. Equation (1) assumes that  $\Delta n_{\text{eff}}/n_{\text{eff}}$  is small and that the bending is a small perturbation on the modal intensity profile of the straight guiding mode. Although more sophisticated methods typically used for calculations of the bending losses, such as beam propagation or mode expansion, become inaccurate for submicron cross-section

high index contrast SOI strip waveguides, estimations shows that for  $R=1\mu\text{m}$  the bending loss in SOI strip waveguide can be expected to be of the order of 0.1dB/turn in good correspondence with the experimentally measured number. These estimations do not include, however, the role of the sidewall surface roughness. Observed dependence of bending loss on polarization indicates that the surface roughness is an important factor defining the losses. Analogous polarization dependence was previously observed in Ref. [8], where it was explained by higher interaction of the TM mode with the surface roughness at the bend.

Table 2. Comparison of bending losses of the TE mode measured in single-mode SOI strip waveguides.

Reference	Height (nm)	Width (nm)	Radius ( $\mu\text{m}$ )	Loss (dB/turn)	Wavelength (nm)	Note
This work	220	445	1	$0.086\pm 0.005$	1500	20 bends
			2	$0.013\pm 0.005$	1500	
			5	$\pm 0.005$	1500	
[11]	300	300	2	0.46	1550	24 bends
			3	0.17	1550	
[9]	320	400	1	$\pm 3$	1550	
[8]	200	500	1	0.5	1540	12 bends, poly-Si
			Resonant	0.3	1540	
[10]	220	400	Resonant	1	1550	2 bends
[12]	340	400	Resonant	1	1550	2 bends

It is seen from the Table 2 that measured bending losses are very low, even smaller than measured in bends employing compact resonant structures [8,10,12]. As it is seen from Fig. 4 another important advantage of simple curved bends in comparison with resonant bend structures is their large bandwidth, from 1200nm to 1550nm. Note also that low bending losses reported here were measured for a simple bend design without any optimization. One of the usual ways to compensate the mode shift at the bend and to decrease the radiation losses is to laterally offset the straight waveguide to achieve better mode matching between the field profiles. This can be easily implemented and may help to further decrease bending losses, especially those losses at the longer wavelengths, close to the waveguide cutoff.

## 5. Conclusion

In conclusion, propagation losses and bending losses were accurately measured in single-mode silicon strip waveguides with 445x220nm cross section processed on a standard 200mm CMOS fabrication line. Propagation losses as small as  $3.6\pm 0.1\text{dB/cm}$  were measured for the TE mode by a cut-back method with a maximum waveguide length of 21mm. Bending losses were found to be below 0.005dB/turn for bending radius of  $R=5\mu\text{m}$ , increasing to  $0.013\pm 0.005\text{dB/turn}$  for  $R=2\mu\text{m}$ . Even for the smallest bending radius of  $R=1\mu\text{m}$  the bending loss is only  $0.086\pm 0.005\text{dB/turn}$ . Further optimization of the processing by for example oxidation smoothing of the sidewalls and optimization of the bend design may allow losses to be reduced still further. These loss figures are useful as a benchmark for further development of silicon microphotonic components and circuits on SOI platform for example arrayed waveguide gratings, ring resonators, as well as photonic crystals and photonic crystal bends

## Acknowledgments

The authors gratefully acknowledge the contributions of the MRL staff at the IBM T. J. Watson facility. The authors are also grateful to G.-L.Bona and N.Moll (IBM Zurich Research Laboratory) for useful discussions.